Instability of the contact line and thickness profiles in vertical oil spreadings

J. GOMBA[1], A. G. GONZÁLEZ*[1], J. DIEZ[1], R. GRATTON[1], L. KONDIC[2]

[1]*INSTITUTO DE FÍSICA ARROYO SECO (IFAS)* - UNIVERSIDAD NACIONAL DEL CENTRO DE LA PROVINCIA DE BUENOS AIRES - PINTO 399 - (7000) - TANDIL – ARGENTINA

[2]*NEW JERSEY INSTITUTE OF TECHNOLOGY (NJIT) – NEWARK, NEW JERSEY, USA.*

Estudiamos la inestabilidad de la línea de contacto del derrame de un volumen constante de aceite siliconado (PDMS) sobre substratos verticales de vidrio. La condición inicial se generó a partir de un filamento horizontal de diámetro típico de algunas décimas de mm y viscosidad 10 Stokes. Se emplean dos métodos de diagnóstico óptico. El primero proporciona el perfil del espesor del líquido a lo largo de una línea prestablecida. El segundo genera la configuración bidimensional del derrame. Mediante estas técnicas se determinan el área de la sección del filamento, la forma aproximada del perfil de espesor, el avance de dedos y valles en función del tiempo y el espectro de Fourier de las ondulaciones que se forman en el frente de avance. Los resultados experimentales se comparan con simulaciones numéricas y con un modelo basado en el análisis lineal de perturbaciones. Este modelo simple proporciona un espectro de Fourier en buen acuerdo con los experimentos, y da una buena estimación de la longitud de onda de máximo crecimiento.

We study the instability of the contact line of the spreading of a constant volume silicon oil (PDMS) on vertical glass substrates. The initial condition is generated from a horizontal filament of typical diameter of several tenths of mm and viscosity 10 Stokes. Two optical diagnostic methods are used. The first one gives the film thickness profile along a prescribed line. The second one produces the bidimensional pattern of the spreading. We use these techniques to determine the cross sectional area of the filament, the approximate shape of the profile, the evolution of fingers and troughs in function of time, and the Fourier spectra of the corrugations of the frontline. The experimental results are compared with numerical simulations and a model based on linear perturbations analysis. This simple model yields a Fourier spectrum in good agreement with experiments, and gives a good estimate of the wavelength corresponding to the maximum growth rate.

I. INTRODUCTION

The scenario where a solid surface is being coated by a thin liquid film is ubiquitous in nature, and it also appears in a variety of technological problems (microchip production and microfluidic devices). Basically, the coating process develops as a balance between viscous and surface tension forces; in some configurations, other body forces (such as gravity, centrifugal[1,2] or thermocapillary[3-5] ones) may also be relevant to drive the flow. Coating flows exhibit two main features: one is the existence of a moving free surface, whose position must be calculated as a consequence of the balance among the driving forces, and the other one is the presence of a moving contact line, which defines the boundary between the coated and the uncoated surface. The combination of these two features may give place to complex topologies of stable or unstable flows, with non-trivial shapes of the free surface and corrugations of the contact line.

Here we concentrate on perhaps the simplest of these problems: the flow of a thin film down a vertical planar substrate. In particular we consider the constant volume (CV) situation, in which a fixed fluid volume is placed at the top of the plate. Previously reported experiments have shown that after some time the initially straight advancing front line, where liquid, gas, and solid phase meet, becomes unstable with respect to transverse perturbations. It is generally accepted that this instability is related to the formation of a capillary ridge, just behind the advancing contact line. However, the analysis of the instability has only been done for the constant flux (CF) case, in which the fluid thickness far behind the contact line is kept constant (thus assuring an unlimited supply of fluid). In this case, the analysis exploits a key feature of CF flow, namely, the translational invariance that allows for a traveling wave solution. In contrast, the CV case looses this property and then the analysis presents additional difficulties, as outlined below. Thus, it is still not clear what determines the long-time nature of the instability, in particular the shape of the patterns and the dominant wavelength of the final pattern.

In recent years many authors have paid attention on this problem. On the experimental side, except by the work by Johnson[6,7], most of the authors have considered CV case. This is understandable considering that CF case involves a more complex setup. It must be noted that, rather than the fluid volume, the cross sectional area of the initial condition is the characteristic parameter of the flow, since the transversal extension is irrelevant as long as it is much larger than the flow extension in the vertical direction. In contrast to most of those experiments, we use here much smaller areas, and thus we deal with micrometric films. We also perform detailed diagnostics of the flow that allow us to describe the free surface topography, thickness profiles along given lines, and Fourier spectrum of the contact line.

In this work we study experimentally and numerically the flow of small volumes of silicon oil (PDMS) which spread down on vertical plates, under complete wetting conditions. The initial condition is a horizontal

* Author to whom correspondece should be addressed.

filament (cross section of the order of 10^{-4} cm^2) placed near the top of a vertical glass plate. The initial straight front line becomes corrugated after some time. The flow evolves by forming well-defined rivulets (called fingers) separated by troughs.

We use two simultaneous optical techniques to analyze the evolution of the instability. The first one is based on the use of an anamorphic processing of a vertical light sheet that passes through the flow region. This technique allows us to obtain the thickness profile, which is particularly important in the early stable stages to measure accurately the cross section of the fluid, and thus its volume. The other technique consists of a schlieren method with an iris diaphragm stopping the deflected rays of an illuminating parallel beam, which allows obtaining most of the relevant features of the instability, such as shape of the contact line and free surface topography. In particular, we obtain for the first time the evolution of the Fourier spectrum of the front line.

The experimental results are compared to our own numerical simulations[8], and good agreement is found. We also develop an analytical model to account for both the linear evolution of the instability. The linear evolution of the modes predicted by this model is in agreement with the experimental Fourier spectrum.

We consider in this paper the data based on a typical case, since a more detailed description of all the experiments performed would require an extensive report.

II. BASIC EQUATIONS

The flow in thin liquid films is described within the lubrication approximation, which yields the following non linear PDE[9] for the fluid thickness $h(x,y,t)$:

$$3\mu\frac{\partial h}{\partial t}+\gamma\nabla\cdot\left(h^3\nabla\nabla^2 h\right)-\rho g\frac{\partial h^3}{\partial x}=0, \qquad (1)$$

where μ is viscosity, γ is surface tension, ρ is density and g is gravity. In Eq. (1) the three terms on the left stand for the viscous, capillary and gravitational forces, respectively.

We have developed a numerical code to solve this equation[8], and we compare its results with experiments. Due to the well known paradox of the contact line (macroscopic divergence of the viscous dissipation rate), all theoretical and computational methods require some regularizing mechanism: either assumption of a thin precursor film in front of the apparent contact line[10-12], or relaxing the no-slip boundary condition at fluid-solid interface[13-15]. We have recently done an extensive analysis of the computational advantages of these regularizing mechanisms applied to the spreading drop problem[16]. In that paper it is shown that the precursor film model performs computationally much better than the various slip models. Hence, we use a precursor film as a regularizing method in this work.

If the second term in Eq. (1) is neglected we obtain the well-known Huppert's solution:

$$h=\left(\frac{\mu x}{\rho g t}\right)^{1/2} \qquad (2)$$

which extends till h reaches $h=h_{end}$ given by

$$h_{end}=\left(\frac{3A\mu}{2\rho g t}\right)^{1/3} \qquad (3)$$

where A is the initial cross section area. This solution approximates the bulk region of the flow provided the size of the frontal region where surface tension effects are important is sufficiently small.

III. EARLY STAGE: ANAMORPHIC LENS TECHNIQUE

The early stages of the spreading, when h is almost independent on the transverse (horizontal) coordinate, are studied by employing the optical system described in Ref. 17. The liquid film is probed by a parallel light sheet at normal incidence with respect to the glass substrate, and elongated in the x (vertical) direction. A lens L of focal length F forms a magnified image of the spreading region on a screen, with a magnification factor M. Then, at the focal plane of L we place an anamorphic lens equivalent to two crossed cylindrical lenses, one convergent and the other divergent, with focal lengths of equal magnitude f, and their axes at ±45° with respect to the x-axis (in fact, a cylindrical-spherical ophthalmic lens, conveniently chosen and oriented, makes this job). Therefore, a bright curve $y_s(x_s)$ appears on the screen, whose coordinates satisfy:

$$x_s=Mx, \quad y_s=M\frac{F^2}{f}(n-1)\frac{\partial h}{\partial x}, \qquad (4)$$

where n is the refraction index of the silicon oil ($=1.4$).

In Fig. 1 we show two images of the curve observed on the screen. They correspond to early stages of the spreading of a filament with an approximate diameter 0.26 mm placed initially near the top of the vertical glass (images are inverted upside down by the optical system).

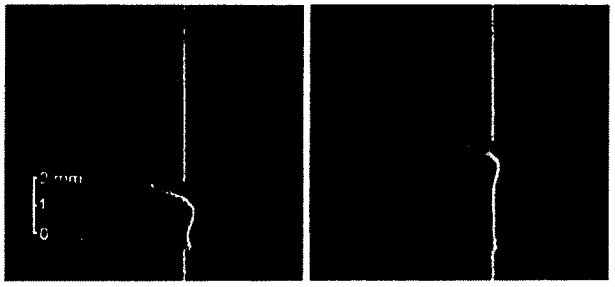

(a) (b)

Fig. 1. Snapshots of the originally vertical light sheet after going through the spreading and the anamorphic system. The thickness gradients along the line are responsible for the horizontal deflections. (a) t=13 min from the beginning of the experiment. Troughs and fingers are not yet well-established (b) t= 51 min after the beginning. It corresponds to a situation where the sheet probes the flow at a trough of the front line.

The integration of the curve $\partial h/\partial x$ vs. x, obtained from Fig 1a, yields the thickness profile $h(x)$ shown in Fig. 2.

Further integration of the profile yields a good estimation of the initial cross section area A of the filament. In this experiment A is $(5.5\pm0.5)10^{-4}$ cm^2. This technique is a valuable tool in analyzing the early stages of the spreading. As soon as the film develops a 2D pattern with transverse gradients, the method becomes more difficult to use except in particular positions with high symmetry, such as troughs or fingers.

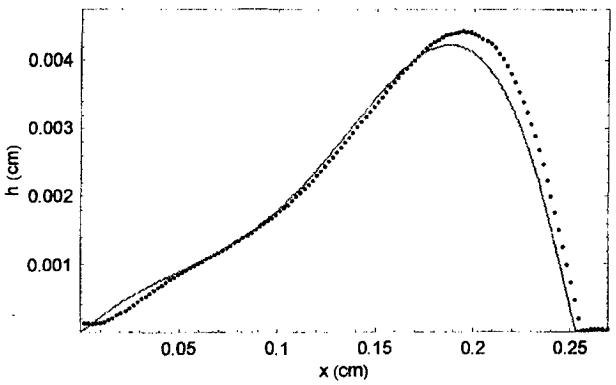

Fig 2. Experimental (dots) and numerical (thick line) film thickness profiles at t=13 min. The experimental points are obtained by using the anamorphic lens technique (Fig 1a).

IV. PERTURBED STATE AND INSTABILITY: SCHLIEREN METHOD

We study the perturbed state by using a schlieren technique with a diaphragm centered at the focus of lens L and an extended probing light beam. The images obtained show a pattern of dark (corresponding to regions where the modulus of the gradient of the thickness is greater than a cutoff value) and bright zones (corresponding to regions where it is smaller). The cutoff value varies with the diameter of the diaphragm. From these patterns it is possible to reconstruct the thickness of the film, although the procedure is a bit cumbersome. In this paper, we restrict our analysis to the study of the shape of the frontline. In Fig. 3 we show four typical images obtained by using this technique. The formation of a pattern of fingers and troughs is clearly shown. By using a discrete Fourier transform, we analyze the spectra of normal modes that correspond to this frontline.

The spectra that correspond to the frontlines at several times are given in Fig. 4. They show a dominant wavelength of approximately 0.6 cm. We postpone a discussion of this result and the evolution of the spectra to the presentation of our model in next section.

In Fig. 5 we show x-positions of the central point of a finger and the central point of an adjacent trough. For comparison, we show also the trajectory of a unperturbed frontline (straight) as given by the numerical simulation (full dark line). The agreement in the early stage is a cross check that the fluid volume has been accurately measured. Fig. 5 also allows estimating the time of the onset of the instability (t≈10 min).

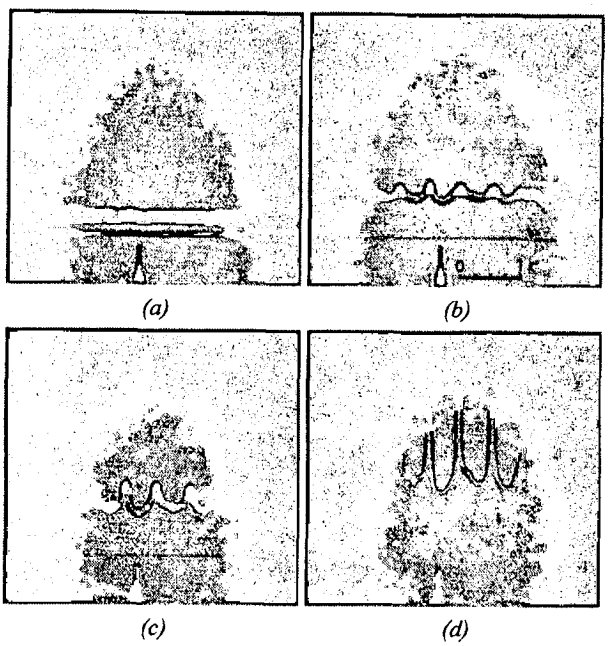

Fig. 3. Evolution of the film using a schlieren technique. The diaphragm has a diameter of 1mm, (a) t= 31 min, (b) t= 123 min, (c) t=189 min, (d) t=1167 min from the beginning. Images are inverted upside down by the optical system

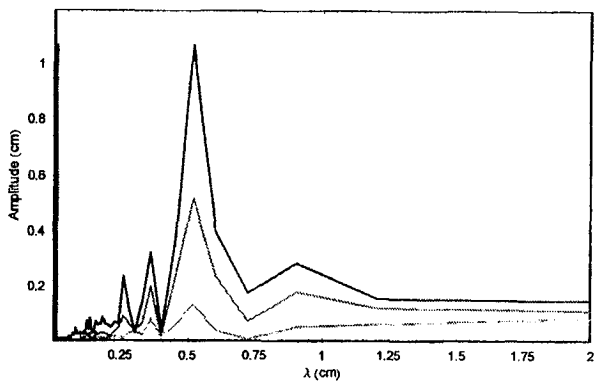

Fig 4. Spectra of the frontline for different times. Lighter gray line corresponds to t=54 min, medium gray line to t=123 min and dark black line to t=189 min.

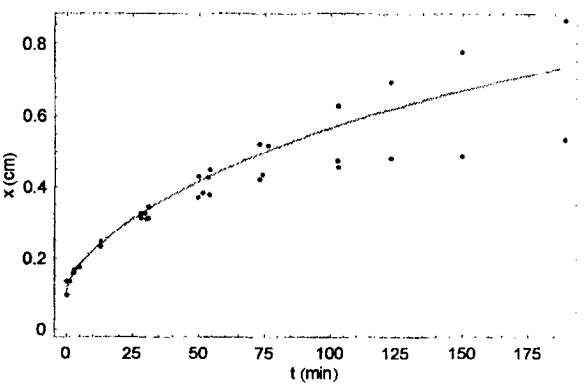

Fig 5: Position of fingers and troughs from experimental data (dots) and evolution of unperturbed frontline from simulation (solid line) corresponding to an experiment with $A= 5.5\ 10^{-4}\ cm^2$.

V. LINEAR STABILITY ANALISIS

Constant flux case (CF)

Thanks to the translational invariance of this case, the solution of the y independent version of Eq. (1) is of the traveling wave type. Thus, for a constant thickness, h_p, in the far region behind the front, we have a dimensionless solution of the form,

$$h = h_p H(\xi), \quad \xi = (x - ut)/\ell, \tag{5}$$

where

$$\ell = \left(a^2 h_p\right)^{1/3}, \quad u = u_0\left(1 + H_f + H_f^2\right), \tag{6}$$

with $u_0=\rho g h_p^2/3\mu$ and $H_f=h_f/h_p$. Here, h_f is the thickness of the precursor film. The main feature of this solution is the presence of the bump in the front region[16]. As it is well known in the literature, this bump is the signature indicating the instability of the solution.

In the linear stability analysis of this problem, it is assumed that the base solution $H(\xi)$ is perturbed with a transverse perturbation characterized by a wavelength λ. Thus, the perturbed solution with normal modes is written as:

$$\tilde{H}(\xi, y, t) = H(\xi) + \varepsilon g(\xi)\cos(ky)\exp(\sigma t), \tag{7}$$

where ε is the (small) amplitude of the perturbation, $g(\xi)$ is the eigenfunction, σ is the growth rate, and $k=2\pi/\lambda$. Interestingly enough, the growth rate can be written as

$$\sigma(q) = \sigma_{max} F(q), \tag{8}$$

where $q=\lambda/\lambda^*$, σ_{max} is the maximum growth rate, and λ^* is the critical wavelength, such that the solution is stable for $q<1$ ($\lambda<\lambda^*$), and unstable otherwise. For instance, in the above-mentioned case, we have $\sigma_{max} \approx 0.285\ u_0/\ell$ and $\lambda^* \approx 7.4\ell$. The function $F(q)$ can be fitted by

$$F(q) = 95 q^2\left(1 - q^{1/17}\right), \tag{9}$$

under the conditions $F(1)=0$ and $F'(q_{max})=0$.

The departures from this function increases as q increases, but the fitting in the unstable range is reasonably good, and will be helpful in the model developed for CV case in the following section.

Constant volume case (CV)

A major hindrance to perform the linear stability analysis of the unperturbed solution $h(x,t)$ for the CV case, is the fact that it is time dependent because the problem does not admit a traveling wave solution unlike the CF case. Basically, this is due to the lost of translational invariance in the present problem. Here, we extend the linear stability analysis of the CF case in an heuristic fashion.

Let us consider a profile $h(x,t_0)$ after the fluid has been released. We assume that at t_0 the flow has evolved enough from the initial condition and has developed a bump in the front region[1]. To perform the analysis, we perturb the solution $h(x,t_0)$ with a transverse corrugation characterized by wavelength λ and initial amplitude $A_0=A(t_0)$. A key point in describing the linear evolution of this small perturbation is to assume that the structure of the thickness profile in the front region is well fitted by the profile of the CF case for $t>t_0$. This implies that a different value of h_p will be appropriate for different times. Under this assumption, Eq. (8) becomes,

$$\sigma(q) = \sigma_{max} h_p^{2/3}(t) F(q), \tag{10}$$

where

$$q = \frac{\lambda^*}{\lambda} h_p^{1/3}(t). \tag{11}$$

Here, $h_p(t)$, λ are expressed in units of the capillary length $a=\sqrt{\gamma/\rho g}$, and σ, t are in units of the time scale $\tau=3\mu a/\rho g$ and τ^{-1}, respectively. Also, since the precursor film of the CF profile (that approximates the CV profile near the bump region) has the same value h_f, the dimensionless thickness in Eq. (6) is $H_f(t)=h_f/h_p(t)$.

The instantaneous growth satisfies $\sigma=A^{-1}dA/dt$, so that we have:

$$A(t) = A_0 \exp\left(\int_{t_0}^{t} \sigma(t')\, dt'\right) \tag{12}$$

Thus, Eqs. (10) and (11) allow us to calculate the instantaneous growth rate of the perturbation as a function of the thickness $h_p(t)$, and Eq. (12) predicts its amplitude.

How the fitting procedure is performed is a critical point of the model. Usually, the approach to this problem has consisted on matching CF solution (also called inner solution) with Huppert's bulk profile (outer solution). However, the matching $h_p=h_{end}$ (that we shall call Huppert's profile model) does not necessarily lead to an appropriate value of the bump thickness h_b, as seen when the result is compared with the numerical solution of the full equation. In this work we find that the instability mechanism is closely related to the height and width of the bump region. Consequently, if the approach fails to yield the right value of h_b, it will certainly lead to inaccurate predictions. Therefore, our approach here is to look for the value of h_p in CF profile, such that the corresponding height of the bump be coincident with the actual value h_b as given by the numerical calculations.

We now proceed to compare the results of the experiment with our model at $t=123$ *min* (see Fig. 6). The model results are based on the linear evolution of the experimental spectrum at $t=t_0=31$ *min*. The agreement between predicted and experimental spectra is remarkably good and both show that the dominant wavelength is close to $\lambda=0.6$ *cm*.

In Fig. 7 we show the same comparison by using Huppert's profile model. This model predicts a less peaked spectrum with lower growth rates. This is due to the fact that the height of the bump is underestimated now. Note that the onset of the instability occurs in our experiment when the parabolic part of the profile pre-

[1] The value of t_0 depends on the shape of initial condition.

dicted by Huppert's solution extends on a small rear fraction of the total width of the spreading.

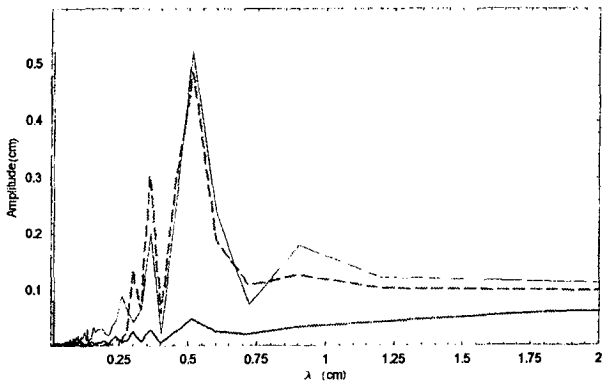

Fig. 6. Spectral evolution of the front line using our model. The lower and upper gray lines correspond to the experimental spectra at t=31min and 123 min, respectively. The dashed line is the spectrum predicted by our model at t=123 min, assuming linear evolution from the spectrum at t=31 min.

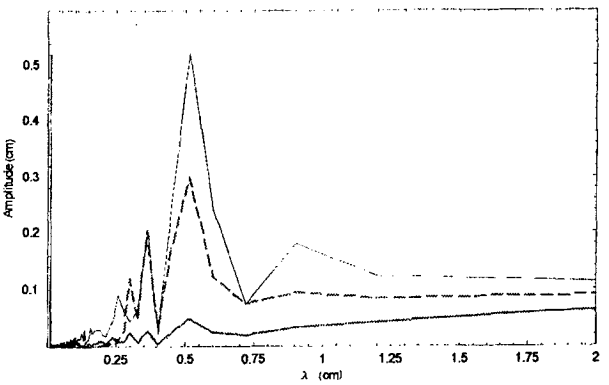

Fig. 7. Idem Fig. 6 but using the Huppert's profile model (dashed line).

VI. CONCLUSIONS

We obtain detailed thickness profiles of the spreading using an optical technique employing an anamorphic system. We apply this technique to the early stages of the experiment, but can also be used to study the profiles in troughs and fingers, although we omit details here for brevity. We compare the experimental data with theoretical results and find them in good agreement. Even though, the experimental profiles in the early stages of a spreading were obtained by Tanner[18] using another technique, no comparison with theoretical models has been reported in the literature.

Previous studies of similar experiments with constant volume, have considered only the mean distance between fingertips. Here we report for the first time a detailed experimental study of the wavelength spectrum of the frontline and its time evolution. Furthermore, we develop a model based on the linear evolution of the instability, which successfully predicts the experimental spectra. The results of our model agree with the experimental data not only by predicting the relevant wavelengths but also the time evolution of the amplitudes of their components.

Based on our more detailed study we conclude that the general ideas, usually reported in the literature, on the ability of a Huppert's profile model to describe the behavior of the instability, do not ensure accurate predictions. Our model, based on considering the bump height, is tested and shown to be very good in describing the time evolution of the instability.

References

1 - N. Fraysse, G. M. Homsy, Phys. Fluids **6**, 1491 (1994)

2 - F. Melo, J. F. Joanny, S. Fauve, Phys. Rev. Lett. **63**, 1958(1989}

3 - A. M. Cazabat, F. Heslot, S. M. Troian, P. Carles, Nature **346**, 824 (1990).

4 - M. J. Tan, S. G. Bankoff, S. H. Davis, Phys. Fluids A **2**, 313 (1990).

5 - X. Fanton, A. M. Cazabat, D. Quéré, Langmuir **12**, 5875 (1996).

6 - M. F. G. Johnson, PhD Thesis, Northwestern University (1997)

7 - M. F. G. Johnson, R. A. Schluter, M. J. Miksis, S. G. Bankoff, J. Fluid Mech. **394**, 339 (1999).

8 - J. Diez, L. Kondic, J. Comp. Phys., in press (2002); L. Kondic, J. Diez, Phys. Fluids **13**, 3168(2001); L. Kondic, J. Diez, Phys. Rev. E **65**, 045301 (2002).

9 - P. G. de Gennes, Rev. Mod. Phys. **57**, 827(1985).

10 - S. M. Troian, E. Herbolzheimer, S. A. Safran, J. F. Joanny, Europhys. Lett. **10**, 25 (1989).

11 - A. L. Bertozzi, M. P. Brenner, Phys. Fluids **9**, 530 (1997).

12 - M. A. Spaid, G. M. Homsy, Phys. Fluids **8**, 460 (1996).

13 - H. P. Greenspan, J. Fluid Mech. **84**, 125 (1978)

14 - E. B. Dussan V., J. Fluid Mech. **77**, 665 (1976).

15 - L. M. Hocking, A. D. Rivers, J. Fluid Mech. **121**, 425 (1982).

16 - J. Diez, L. Kondic, A. L. Bertozzi, Phys. Rev. E **63**, 011208 (2001).

17 - L. Thomas, R. Gratton, B. Marino, S. Betelu, J. Diez, J. Simon, Meas. Sci. Technol. **7**, 1134 (1996).

18 - L. H. Tanner, Optical and Laser Technology, pages 125-128 (1978)